

Relaying Protocols for Wireless Energy Harvesting and Information Processing

Ali A. Nasir, *Student Member, IEEE*, Xiangyun Zhou, *Member, IEEE*,

Salman Durrani, *Senior Member, IEEE*, and Rodney A. Kennedy, *Fellow, IEEE*

Abstract

An emerging solution for prolonging the lifetime of energy constrained relay nodes in wireless networks is to avail the ambient radio-frequency (RF) signal and to simultaneously harvest energy and process information. In this paper, an amplify-and-forward relaying network is considered, where an energy constrained relay node harvests energy from the received RF signal and uses that harvested energy to forward the source information to the destination. Based on the time switching and power splitting receiver architectures, two relaying protocols, namely, i) time switching-based relaying (TSR) protocol and ii) power splitting-based relaying (PSR) protocol are proposed to enable energy harvesting and information processing at the relay. In order to determine the throughput, analytical expressions for outage probability and ergodic capacity are derived for delay-limited and delay-tolerant transmission modes, respectively. The numerical analysis provides practical insights into the effect of various system parameters, such as energy harvesting time, power splitting ratio, source transmission rate, source to relay distance, noise power, and energy harvesting efficiency, on the performance of wireless energy harvesting and information processing using AF relay nodes. In particular, the TSR protocol outperforms the PSR protocol in terms of throughput at relatively low signal-to-noise-ratios and high transmission rate.

Index Terms

Energy harvesting, wireless energy transfer, amplify-and-forward, cooperative systems, throughput, outage probability, ergodic capacity.

Ali A. Nasir, Xiangyun Zhou, Salman Durrani, and Rodney Kennedy are with Research School of Engineering, The Australian National University, Australia. Emails: ali.nasir@anu.edu.au, xiangyun.zhou@anu.edu.au, salman.durrani@anu.edu.au, and rodney.kennedy@anu.edu.au. This research was supported under Australian Research Council's Discovery Projects funding scheme (project number DP110102548).

I. INTRODUCTION

Prolonging the lifetime of a wireless network through energy harvesting has received significant attention very recently [1]–[12]. Though, replacing or recharging batteries can avoid energy harvesting, it incurs a high cost and can be inconvenient or hazardous (e.g., in a toxic environments), or highly undesirable (e.g., for sensors embedded in building structures or inside the human body) [12]. In such scenarios, a safe and convenient option may be to harvest energy from the environment. Apart from the conventional energy harvesting methods, such as solar, wind, vibration, thermoelectric effects or other physical phenomena [1]–[3], [9], [13]–[15], a new emerging solution is to avail ambient radio-frequency (RF) signals [4]. The advantage of this solution lies in the fact that RF signals can carry energy and information at the same time. Thus, energy constrained nodes can scavenge energy and process the information simultaneously [4]–[7], [10], [12].

For wireless energy harvesting using RF signals, the recent state-of-the-art advances in point-to-point systems can be classified into two main approaches. The first approach proposes an ideal receiver design that is able to simultaneously observe and extract power from the same received signal [4], [5], [10]. However, as discussed in [6], this assumption may not hold in practice, as practical circuits for harvesting energy from RF signals are not yet able to decode the carried information directly. The second approach considers a more practical receiver design with separate information decoding and energy harvesting receiver for information and power transfer [6], [11], [12], [16], [17]. For the first class of receivers, the idea of transmitting information and energy simultaneously was first proposed in [4], where the authors used a capacity-energy function to study the fundamental performance tradeoff for simultaneous information and power transfer. The work in [4] was extended to frequency-selective channels with additive white Gaussian noise (AWGN) in [5]. A two-way communication system for energy harvesting and information transmission was investigated in [10]. For the second class of receivers, the performance limits of a three node multiple-input-multiple-output (MIMO) broadcasting system, with separate energy harvesting and information decoding receiver, was studied in [12]. The work in [12] was extended in [16] by considering imperfect channel state information (CSI) at the transmitter. Subject to co-channel interference, optimal

designs to achieve different outage-energy and rate-energy tradeoffs in delay-limited and delay-tolerant transmission modes were formulated in [11]. The application of wireless energy harvesting to a cognitive radio network was considered in [17], where the throughput of the secondary network was maximized under an outage constraint for primary and secondary networks.

A. Motivation and Contribution

The majority of the recent research in wireless energy harvesting and information processing has considered point-to-point communication system [4]–[6], [10]–[12], [16], [17]. In wireless cooperative or sensor networks, relay or sensor nodes may have limited battery reserves and need to rely on some external charging mechanism in order to remain active and forward messages to other nodes [15], [18]. Therefore, energy harvesting in such networks is particularly important as it can enable information relaying.

In this paper, we are concerned with the problem of wireless energy harvesting and information processing in an amplify-and-forward (AF) wireless cooperative or sensor network. We consider the scenario that an energy constrained relay node harvests energy from the RF signal broadcasted by a source node and uses that harvested energy to forward the source signal to a destination node. We adopt time switching (TS) and power splitting (PS) receiver architectures, as proposed in [6]. Based on these receiver architectures, we propose two relaying protocols i) TS-based relaying (TSR) protocol and ii) PS-based relaying (PSR) protocol for separate information processing and energy harvesting at the energy constrained relay node. In TSR protocol, the relay spends some time for energy harvesting and the remaining time for information processing. In PSR protocol, the relay uses portion of the received power for energy harvesting and the remaining power for information processing. Our figure of merit is the throughput, which is defined as the number of bits that are successfully decoded per unit time per unit bandwidth at the destination node. We formulate and study the throughput for both TSR and PSR protocols with delay-limited and delay-tolerant transmission modes, where outage probability and ergodic capacity are derived to evaluate the throughput in delay-limited and delay-tolerant transmission modes, respectively. The main contributions of this paper are summarized as follows:

- We propose the TSR and PSR protocols to enable wireless energy harvesting and information processing at the energy constrained relay in wireless AF relaying networks, based on the TS and PS receiver architectures.
- For TSR and PSR protocols, we derive analytical expressions for the achievable throughput at the destination by i) evaluating the outage probability for delay-limited transmission mode and ii) evaluating the ergodic capacity for delay-tolerant transmission mode. The derived expressions provide practical design insights into the effect of various system parameters.
- Comparing TSR and PSR protocols, our numerical analysis shows that in delay-limited transmission mode, the throughput performance of TSR protocol is superior to PSR protocol at higher transmission rates, at relatively lower signal-to-noise-ratio (SNR), and for lower energy harvesting efficiency. This is in contrast with point-to-point system where the PS receiver architecture always achieve larger rate-energy pairs than the TS receiver architecture.
- For both TSR and PSR protocols, our numerical results show that locating the relay node closer to the source node yields larger throughput in delay-limited and delay-tolerant transmission modes. This is also in contrast with the general case where energy harvesting is not considered at the relay and the maximum throughput results when the relay is located midway between the source and destination.

B. Related Works

Some recent studies have considered energy harvesting through RF signals in wireless cooperative networks [7], [8]. In [8], the authors considered a MIMO relay system and studied different tradeoffs between the energy transfer and the information rates to achieve optimal source and relay precoding. However, the authors in [8] assume that the relay has its own internal energy source and does not need external charging. In contrast to [8], we consider the case that the relay relies on external charging through RF signal from the source node. In [7], the authors investigated multi-user and multi-hop systems for simultaneous information and power transfer. It was shown in [7] that for a dual-hop channel with an energy harvesting relay, the transmission strategy depends on the quality of the second link. However, in [7], the optimization strategy assumed perfect channel state information at the transmitter, which is often

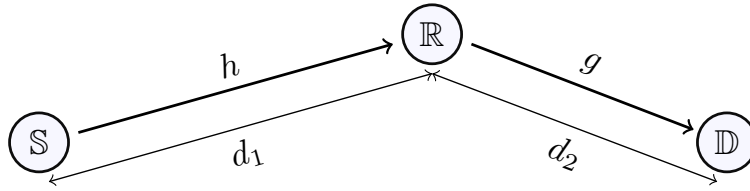


Fig. 1. System model for energy constrained relay assisted communication between a source and a destination node.

not practical. Further, it is assumed in [7] that relay node is able to decode information and extract power simultaneously, which, as explained in [6], may not hold in practice. In contrast to [7], the system model proposed in this paper assumes the availability of the channel state information at the destination only and adopts the practical receiver architecture at the relay with separate information decoding and energy harvesting.

C. Organization

The remainder of the paper is organized as follows: Section II presents the overall system model and assumptions. Sections III and IV detail the TSR and PSR protocols, respectively, and analytically characterize the throughput performance. Section V presents the numerical results from which various design insights are obtained. Finally, Section VI concludes the paper and summarizes the key findings.

II. SYSTEM MODEL

A wireless communication system is considered, where information is transferred from the source node, \mathbb{S} , to the destination node, \mathbb{D} , through an energy constrained intermediate relay node, \mathbb{R} . Fig. 1 shows the system model for the considered system. The channel gains from the source to relay and the relay to destination nodes are denoted by h and g , respectively. The distances from the source to relay and the relay to destination nodes are denoted by d_1 and d_2 , respectively. Throughout this paper, the following set of assumptions are considered.

- A1. There is no direct link between the source and the destination node. Thus, an intermediate relay assists the transmission of source messages to the destination [19]. A single relay node is considered for simplicity as shown in Fig. 1.

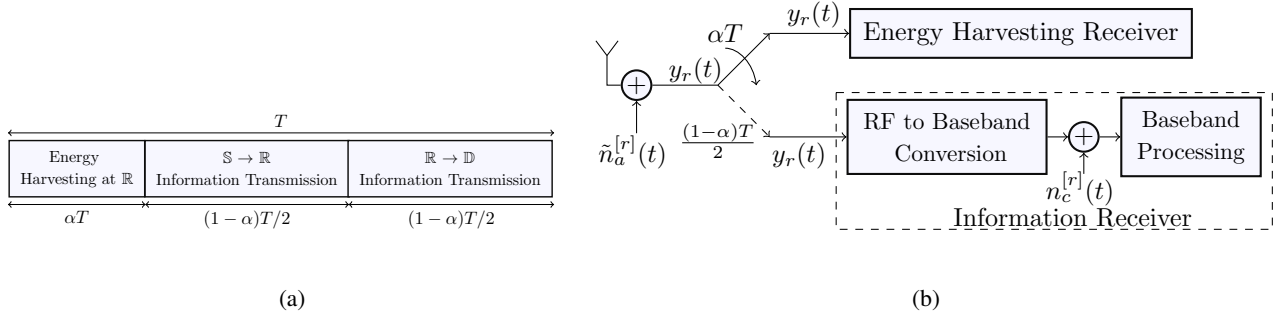


Fig. 2. (a) Illustration of key parameters in the TSR protocol for energy harvesting and information processing at the relay. (b) Block diagram of the relay receiver in the TSR protocol.

- A2. The intermediate relay is an energy constrained node. It first harvests energy from the source signal. Then, it uses the harvested energy as a source of transmit power to forward the source information to the destination.
- A3. Amongst the different relaying protocols, amplify-and-forward (AF) scheme is chosen at the relay node due to its implementation simplicity [20].
- A4. It is assumed that the processing power at the relay node is negligible as compared to the power used for signal transmission from the relay to the destination. This assumption is inline with [6].
- A5. The channel gains, h and g are modeled as quasi-static, independent and identically distributed (i.i.d.) frequency-flat Rayleigh fading parameters. The use of such channels is motivated by prior research in this field [2], [3], [6], [11], [12], [15]. Further, it is assumed that the channel state information is known only at the destination.

Based on the time switching and power splitting receiver architectures, we propose two relaying protocols to harvest energy from the source RF signal, i) TSR protocol and ii) PSR protocol, which are described and analyzed in detail in the following sections.

III. TIME SWITCHING-BASED RELAYING (TSR) PROTOCOL

Fig. 2(a) depicts the key parameters in the TSR protocol for energy harvesting and information processing at the relay. In Fig. 2(a), T is the *block time* in which a certain block of information is transmitted from the source node to the destination node and α is the fraction of the block time in which relay harvests energy from the source signal, where $0 \leq \alpha \leq 1$. The remaining block time, $(1 - \alpha)T$ is used

for information transmission, such that half of that, $(1 - \alpha)T/2$, is used for source to relay information transmission and the remaining half, $(1 - \alpha)T/2$, is used for relay to destination information transmission. The choice of the time fraction, α , used for harvesting energy at the relay node, affects the achievable throughput at the destination. The following subsections analyze the energy harvesting and information processing at the relay node.

A. Energy Harvesting

The block diagram for the relay receiver in the TSR protocol is shown in Fig. 2(b). The RF signal, $y(t)$ received at the relay node is first sent to the *energy harvesting receiver* (for αT time) and then to the *information receiver* (for $(1 - \alpha)T/2$ time). Note that the RF signal, $y(t)$ is corrupted by the narrow-band Gaussian noise, $\tilde{n}_a^{[r]}(t)$, introduced by the receiving antenna.¹ The energy harvesting receiver rectifies the RF signal directly and gets direct current to charge up the battery. The details of such an energy harvesting receiver can be found in [6]. As shown in Fig. 2(b), the received signal at the relay node, $y_r(t)$ is given by

$$y_r(t) = \frac{1}{\sqrt{d_1^m}} \sqrt{P_s} h s(t) + \tilde{n}_a^{[r]}(t), \quad (1)$$

where h is the source to relay channel gain, d_1 is the source to relay distance, P_s is the transmitted power from the source, m is the path loss exponent, and $s(t)$ is the normalized information signal from the source, i.e., $\mathbb{E}\{|s(t)|^2\} = 1$, where $\mathbb{E}\{\cdot\}$ is the expectation operator and $|\cdot|$ is the absolute value operator.

Using (1), the harvested energy, E_h during energy harvesting time αT is given by [6]

$$E_h = \frac{\eta P_s |h|^2}{d_1^m} \alpha T, \quad (2)$$

where $0 < \eta < 1$ is the energy conversion efficiency.

B. Energy constrained Relay-Assisted Transmission

The information receiver in Fig. 2(b) down-converts the RF signal to baseband and processes the baseband signal, where $n_c^{[r]}(t)$ is the additive noise due to RF band to baseband signal conversion. After

¹Note that the superscript $[r]$, e.g., with the noise $\tilde{n}_a^{[r]}(t)$, is used to indicate the noise at the relay node.

down conversion, the sampled baseband signal at the relay node, $y_r(k)$, is given by

$$y_r(k) = \frac{1}{\sqrt{d_1^m}} \sqrt{P_s} h s(k) + n_a^{[r]}(k) + n_c^{[r]}(k), \quad (3)$$

where k denotes the symbol index, $s(k)$ is the sampled and normalized information signal from the source, $n_a^{[r]}(k)$ is the baseband additive white Gaussian noise (AWGN) due to the receiving antenna at the relay node,² and $n_c^{[r]}(k)$ is the sampled AWGN due to RF band to baseband signal conversion. The relay amplifies the received signal and the transmitted signal from the relay, $x_r(k)$ is given by

$$x_r(k) = \frac{\sqrt{P_r} y_r(k)}{\sqrt{\frac{P_s |h|^2}{d_1^m} + \sigma_{n_a^{[r]}}^2 + \sigma_{n_c^{[r]}}^2}}, \quad (4)$$

where the factor in the denominator, $\sqrt{\frac{P_s |h|^2}{d_1^m} + \sigma_{n_a^{[r]}}^2 + \sigma_{n_c^{[r]}}^2}$ is the power constraint factor at the relay, $\sigma_{n_a^{[r]}}^2$ and $\sigma_{n_c^{[r]}}^2$ are the variances of the AWGNs, $n_a^{[r]}(k)$ and $n_c^{[r]}(k)$, respectively, and P_r is the power transmitted from the relay node. The transmitted power, P_r depends on the harvested energy at the relay during energy harvesting time. The sampled received signal at the destination, $y_d(k)$ is given by

$$y_d(k) = \frac{1}{\sqrt{d_2^m}} g x_r(k) + n_a^{[d]}(k) + n_c^{[d]}(k), \quad (5)$$

where $n_a^{[d]}(k)$ and $n_c^{[d]}(k)$ are the antenna and conversion AWGNs at the destination node, respectively, and g is the relay to destination channel gain. Substituting (4) into (5), we have

$$y_d(k) = \frac{g \sqrt{P_r d_1^m} y_r(k)}{\sqrt{d_2^m} \sqrt{\frac{P_s |h|^2}{d_1^m} + \sigma_{n_a^{[r]}}^2 + \sigma_{n_c^{[r]}}^2}} + n_a^{[d]}(k) + n_c^{[d]}(k). \quad (6)$$

Finally, substituting $x_r(k)$ from (3) into (6), $y_d(k)$ is given by

$$y_d(k) = \frac{\sqrt{P_r P_s} h g s(k)}{\sqrt{d_2^m} \sqrt{P_s |h|^2 + d_1^m \sigma_{n^{[r]}}^2}} + \frac{\sqrt{P_r d_1^m} g n^{[r]}(k)}{\sqrt{d_2^m} \sqrt{P_s |h|^2 + d_1^m \sigma_{n^{[r]}}^2}} + n^{[d]}(k), \quad (7)$$

where $n^{[r]}(k) \triangleq n_a^{[r]}(k) + n_c^{[r]}(k)$ and $n^{[d]}(k) \triangleq n_a^{[d]}(k) + n_c^{[d]}(k)$ are the overall AWGNs at the relay and destination nodes, respectively and $\sigma_{n^{[r]}}^2 \triangleq \sigma_{n_a^{[r]}}^2 + \sigma_{n_c^{[r]}}^2$. Using E_h in (2), the transmitted power from the relay node, P_r is given by

$$P_r = \frac{E_h}{(1 - \alpha)T/2} = \frac{2\eta P_s |h|^2 \alpha}{d_1^m (1 - \alpha)}, \quad (8)$$

²Note that $n_a^{[r]}(k)$ is the baseband equivalent noise of the pass band noise $\tilde{n}_a^{[r]}(t)$ [6].

where (8) follows from the fact that relay communicates with the destination node for the time $(1-\alpha)T/2$, as shown in Fig. 2(a). Substituting the value of P_r from (8) into (7), the received signal at the destination, $y_d(k)$ in terms of P_s , η , α , d_1 and d_2 , is given by

$$y_d(k) = \underbrace{\frac{\sqrt{2\eta|h|^2\alpha}P_s h g s(k)}{\sqrt{(1-\alpha)d_1^m d_2^m} \sqrt{P_s|h|^2 + d_1^m \sigma_{n[r]}^2}}}_{\text{signal part}} + \underbrace{\frac{\sqrt{2\eta P_s|h|^2\alpha} g n^{[r]}(k)}{\sqrt{(1-\alpha)d_2^m} \sqrt{P_s|h|^2 + d_1^m \sigma_{n[r]}^2}}}_{\text{overall noise}} + n^{[d]}(k). \quad (9)$$

C. Throughput Analysis

Using (9), the signal-to-noise-ratio (SNR) at the destination node, γ_D is given by

$$\begin{aligned} \gamma_D &= \frac{\frac{2\eta P_s^2 |h|^4 |g|^2 \alpha}{(1-\alpha)d_1^m d_2^m (P_s|h|^2 + d_1^m \sigma_{n[r]}^2)}}{\frac{2\eta P_s |h|^2 |g|^2 \sigma_{n[r]}^2 \alpha}{(1-\alpha)d_2^m (P_s|h|^2 + d_1^m \sigma_{n[r]}^2)} + \sigma_{n[d]}^2} \\ &= \frac{2\eta P_s^2 |h|^4 |g|^2 \alpha}{2\eta P_s |h|^2 |g|^2 d_1^m \sigma_{n[r]}^2 \alpha + P_s |h|^2 d_1^m d_2^m \sigma_{n[d]}^2 (1-\alpha) + d_1^{2m} d_2^m \sigma_{n[r]}^2 \sigma_{n[d]}^2 (1-\alpha)}, \end{aligned} \quad (10)$$

where $\sigma_{n[d]}^2 \triangleq \sigma_{n_a[d]}^2 + \sigma_{n_c[d]}^2$. In the following, the throughput, τ , is determined at the destination node, given the received SNR, γ_D in (10), for both delay-limited and delay-tolerant transmission modes.

1) Delay-limited Transmission: In delay-limited transmission mode, throughput is determined by evaluating the outage probability, p_{out} , at a fixed source transmission rate, i.e., R bits/sec/Hz, where $R \triangleq \log_2(1 + \gamma_0)$ and γ_0 is the threshold value of SNR for correct data detection at the destination. Thus, p_{out} is given by

$$p_{\text{out}} = p(\gamma_D < \gamma_0), \quad (11)$$

where $\gamma_0 = 2^R - 1$. The analytical expression for p_{out} is given in the following proposition.

Proposition 1: The outage probability at the destination node for the TSR protocol is given by

$$p_{\text{out}} = 1 - \frac{1}{\lambda_h} \int_{z=d/c}^{\infty} e^{-\left(\frac{z}{\lambda_h} + \frac{az+b}{(cz^2-dz)\lambda_g}\right)} dz \quad (12a)$$

$$\approx 1 - e^{-\frac{d}{c\lambda_h}} u K_1(u), \quad (\text{high SNR approximation}) \quad (12b)$$

where,

$$a \triangleq P_s d_1^m d_2^m \sigma_{n[d]}^2 \gamma_0 (1 - \alpha), \quad (13a)$$

$$b \triangleq d_1^{2m} d_2^m \sigma_{n[r]}^2 \sigma_{n[d]}^2 \gamma_0 (1 - \alpha), \quad (13b)$$

$$c \triangleq 2\eta P_s^2 \alpha, \quad (13c)$$

$$d \triangleq 2\eta P_s d_1^m \sigma_{n[r]}^2 \gamma_0 \alpha, \quad (13d)$$

$$u \triangleq \sqrt{\frac{4a}{c\lambda_h\lambda_g}}, \quad (13e)$$

λ_h and λ_g are the mean values of the exponential random variables $|h|^2$ and $|g|^2$, respectively, and $K_1(\cdot)$ is the first-order modified Bessel function of the second kind [21].

Proof: See Appendix A.

Given that the transmitter is communicating R bits/sec/Hz and $(1 - \alpha)T/2$ is the effective communication time from source node to the destination node in the block of time T seconds, as shown in Fig. 2(a), the throughput, τ at the destination is given by

$$\tau = (1 - p_{\text{out}})R \frac{(1 - \alpha)T/2}{T} = \frac{(1 - p_{\text{out}})R(1 - \alpha)}{2}, \quad (14)$$

where the throughput, τ in (14), depends on P_s , η , α , d_1 , d_2 , R , $\sigma_{n[r]}^2$ and $\sigma_{n[d]}^2$.

2) *Delay-Tolerant Transmission:* In delay-tolerant transmission mode, throughput is determined by evaluating the ergodic capacity, C at the destination. Unlike in delay-limited transmission mode, where source transmits at fixed rate R in order to meet some outage criteria, the source can transmit data at any rate less than or equal to the evaluated ergodic capacity, C in delay-tolerant transmission mode. Using the received SNR at the destination, γ_D in (10), C is given by

$$C = \mathbb{E}_{h,g} \{ \log_2(1 + \gamma_D) \}, \quad (15)$$

where γ_D depends on the random channel gains, h and g .

Proposition 2: The ergodic capacity at the destination node for the TSR protocol is given by

$$C = \int_{\gamma=0}^{\infty} \int_{z=d/c}^{\infty} \frac{(az + b)cz^2}{(cz^2 - dz)^2 \lambda_g \lambda_h \gamma} e^{-\left(\frac{z}{\lambda_h} + \frac{az+b}{(cz^2-dz)\lambda_g}\right)} \log_2(1 + \gamma) dz d\gamma \quad (16a)$$

$$\approx \int_{\gamma=0}^{\infty} \left(\frac{u^2 K_0(u) e^{-\frac{d}{c\lambda_h}}}{2\gamma} + \frac{du K_1(u) e^{-\frac{d}{c\lambda_h}}}{\gamma c \lambda_h} \right) \log_2(1 + \gamma) d\gamma, \quad (\text{high SNR approximation}) \quad (16b)$$

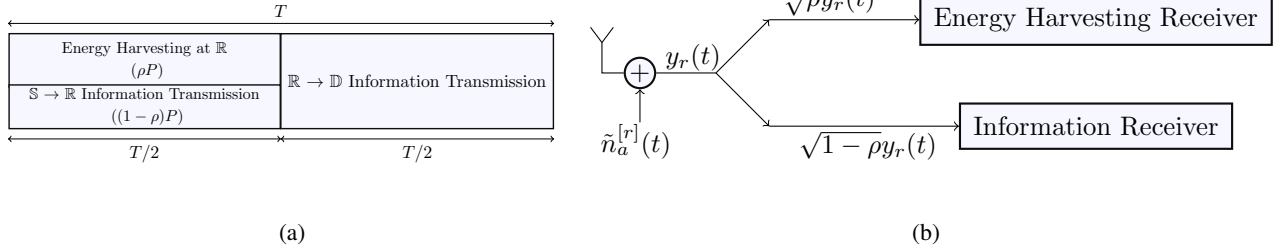


Fig. 3. (a) Illustration of key parameters in the PSR protocol for energy harvesting and information processing at the relay. (b) Block diagram of the relay receiver in the PSR protocol (the details of information receiver are the same as shown in Fig. 2(b)).

where,

$$a \triangleq P_s d_1^m d_2^m \sigma_{n[d]}^2 \gamma (1 - \alpha), \quad (17a)$$

$$b \triangleq d_1^{2m} d_2^m \sigma_{n[r]}^2 \sigma_{n[d]}^2 \gamma (1 - \alpha), \quad (17b)$$

$$c \triangleq 2\eta P_s^2 \alpha, \quad (17c)$$

$$d \triangleq 2\eta P_s d_1^m \sigma_{n[r]}^2 \gamma \alpha, \quad (17d)$$

$$u \triangleq \sqrt{\frac{4a}{c\lambda_h\lambda_g}}, \quad (17e)$$

and λ_h and λ_g are defined below (12).

Proof: See Appendix B.

Note that $(1 - \alpha)T/2$ is the effective communication time between the source node and the destination node in the block of time T seconds, as shown in Fig. 2(a). Assuming that the source is transmitting at a rate equal to the ergodic capacity, i.e., C bits/sec/Hz, the throughput, τ at the destination is given by

$$\tau = \frac{(1 - \alpha)T/2}{T} C = \frac{(1 - \alpha)}{2} C, \quad (18)$$

where the throughput, τ in (18) depends on P_s , η , α , d_1 , d_2 , $\sigma_{n[r]}^2$ and $\sigma_{n[d]}^2$.

IV. POWER SPLITTING-BASED RELAYING (PSR) PROTOCOL

Fig. 3(a) shows the communication block diagram employing the PSR protocol for energy harvesting and information processing at the relay. In Fig. 3(a), P is the power of the received signal, $y_r(t)$ at the relay and T is the total block time, from which half of the time, $T/2$ is used for source to relay information transmission and the remaining half, $T/2$ is used for relay to destination information transmission. During

the first half of the block time, the fraction of the received signal power, ρP is used for energy harvesting and the remaining received power, $(1 - \rho)P$ is used for the source to relay information transmission, where $0 \leq \rho \leq 1$. The choice of the power fraction, ρ , used for harvesting energy at the relay node, affects the achievable throughput at the destination. The following subsections analyze the energy harvesting and information processing at the relay for the PSR protocol.

A. Energy Harvesting

The block diagram for the relay receiver in the PSR protocol is shown in Fig. 3(b). The power splitter splits the received signal in $\rho : 1 - \rho$ proportion, such that the portion of the received signal, $\sqrt{\rho}y_r(t)$ is sent to the energy harvesting receiver and the remaining signal strength, $\sqrt{1 - \rho}y_r(t)$ drives the information receiver. Using the signal received at the input of the energy harvesting receiver, $\sqrt{\rho}y_r(t) = \frac{1}{\sqrt{d_1^m}}\sqrt{\rho P_s}hs(t) + \sqrt{\rho}\tilde{n}_a^{[r]}(t)$, the harvested energy, E_h at the relay is given by [6]

$$E_h = \frac{\eta \rho P_s |h|^2}{d_1^m} (T/2), \quad (19)$$

where energy is harvested at the relay during half of the block time, $T/2$, as shown in Fig. 3(a), and $0 < \eta < 1$ is the energy conversion efficiency.

B. Energy constrained Relay-Assisted Transmission

The block level description of the information receiver in Fig. 3(b) is same as detailed in Fig. 2(b). After down conversion, the sampled baseband signal, $y_r(k)$, at the input of basedband processor in the PSR protocol is given by

$$y_r(k) = \frac{1}{\sqrt{d_1^m}} \sqrt{(1 - \rho)P_s}hs(k) + \sqrt{(1 - \rho)}n_a^{[r]}(k) + n_c^{[r]}(k), \quad (20)$$

where $s(k)$, h , P_s , $n_a^{[r]}(k)$, and $n_c^{[r]}(k)$ are defined below (3) and ρ is the portion of the received power used for energy harvesting, as explained at the start of Section IV. The relay amplifies the received signal and the transmitted signal from the relay is given by

$$x_r(k) = \frac{\sqrt{P_r}y_r(k)}{\sqrt{(1 - \rho)\frac{P_s|h|^2}{d_1^m} + (1 - \rho)\sigma_{n_a^{[r]}}^2 + \sigma_{n_c^{[r]}}^2}}, \quad (21)$$

where the factor in the denominator, $\sqrt{(1-\rho)\frac{P_s|h|^2}{d_1^m} + (1-\rho)\sigma_{n_a}^2 + \sigma_{n_c}^2}$ is the power constraint factor at the relay, P_r is the power transmitted from the relay and $\sigma_{n_a}^2$ and $\sigma_{n_c}^2$ are defined below (4). Substituting (21) into (5), the sampled received signal at the destination node, $y_d(k)$ in the PSR protocol is given by

$$y_d(k) = \frac{g\sqrt{P_r d_1^m} y_r(k)}{\sqrt{d_2^m} \sqrt{(1-\rho)P_s|h|^2 + d_1^m((1-\rho)\sigma_{n_a}^2 + \sigma_{n_c}^2)}} + n_a^{[d]}(k) + n_c^{[d]}(k). \quad (22)$$

Finally, substituting (20) into (22), $y_d(k)$ is given by

$$y_d(k) = \frac{\sqrt{(1-\rho)P_s P_r} h g s(k)}{\sqrt{d_2^m} \sqrt{(1-\rho)P_s|h|^2 + d_1^m \sigma_{n[r]}^2}} + \frac{\sqrt{P_r d_1^m} g n^{[r]}(k)}{\sqrt{d_2^m} \sqrt{(1-\rho)P_s|h|^2 + d_1^m \sigma_{n[r]}^2}} + n^{[d]}(k), \quad (23)$$

where $n^{[r]}(k) \triangleq \sqrt{1-\rho}n_a^{[r]}(k) + n_c^{[r]}(k)$ and $n^{[d]}(k) \triangleq n_a^{[d]}(k) + n_c^{[d]}(k)$ are the overall AWGNs at the relay and destination nodes, respectively and $\sigma_{n[r]}^2 \triangleq (1-\rho)\sigma_{n_a}^2 + \sigma_{n_c}^2$. Note that the definitions of $n^{[r]}(k)$ and $\sigma_{n[r]}^2$ in the PSR protocol are different from the TSR protocol. Using E_h in (19), the transmitted power from the relay node, P_r is given by

$$P_r = \frac{E_h}{T/2} = \frac{\eta P_s |h|^2 \rho}{d_1^m}, \quad (24)$$

where (24) follows from the fact that the relay communicates with the destination node for half of the block time $T/2$, as shown in Fig. 3(a). Substituting the value of P_r from (24) into (23), the received signal at the destination, $y_d(k)$ in terms of P_s , η , ρ , d_1 and d_2 , is given by

$$y_d(k) = \underbrace{\frac{\sqrt{\eta|h|^2 \rho(1-\rho)} P_s h g s(k)}{\sqrt{d_1^m d_2^m} \sqrt{P_s|h|^2(1-\rho) + d_1^m \sigma_{n[r]}^2}}}_{\text{signal part}} + \underbrace{\frac{\sqrt{\eta P_s |h|^2 \rho} g n^{[r]}(k)}{\sqrt{d_2^m} \sqrt{P_s|h|^2(1-\rho) + d_1^m \sigma_{n[r]}^2}}}_{\text{overall noise}} + n^{[d]}(k). \quad (25)$$

C. Throughput Analysis

Using (25), the signal-to-noise-ratio (SNR) at the destination node, γ_D in case of the PSR protocol is given by

$$\gamma_D = \frac{\eta P_s^2 |h|^4 |g|^2 \rho (1-\rho)}{\eta P_s |h|^2 |g|^2 d_1^m \sigma_{n[r]}^2 \rho + P_s |h|^2 d_1^m d_2^m \sigma_{n[d]}^2 (1-\rho) + d_1^{2m} d_2^m \sigma_{n[r]}^2 \sigma_{n[d]}^2} \quad (26)$$

where $\sigma_{n[d]}^2 \triangleq \sigma_{n_a}^2 + \sigma_{n_c}^2$. In the following, we determine the throughput, τ , at the destination node for the PSR protocol, given the received SNR, γ_D in (26), for both delay-limited and delay-tolerant transmission modes.

1) *Delay-Limited Transmission*: Given that the transmitter is communicating R bits/sec/Hz and $T/2$ is the effective communication time from source node to the destination node in the block of time T seconds, as shown in Fig. 3(a), the throughput, τ at the destination node in delay-limited transmission mode is given by

$$\tau = (1 - p_{\text{out}})R \frac{T/2}{T} = \frac{(1 - p_{\text{out}})R}{2} \quad (27)$$

where the outage probability, p_{out} can be calculated using Proposition 3 (see below) for γ_D given in (26) and γ_0 defined below (11).

Proposition 3: For the PSR protocol, p_{out} can be analytically calculated using (12), where³

$$a \triangleq P_s d_1^m d_2^m \sigma_{n[d]}^2 \gamma_0 (1 - \rho), \quad (28a)$$

$$b \triangleq d_1^{2m} d_2^m \sigma_{n[r]}^2 \sigma_{n[d]}^2 \gamma_0, \quad (28b)$$

$$c \triangleq \eta P_s^2 \rho (1 - \rho), \quad (28c)$$

$$d \triangleq \eta P_s d_1^m \sigma_{n[r]}^2 \gamma_0 \rho, \quad \text{and} \quad (28d)$$

$$u \triangleq \sqrt{\frac{4a}{c\lambda_h\lambda_g}}. \quad (28e)$$

The throughput, τ in (27) thus depends on P_s , η , ρ , d_1 , d_2 , R , $\sigma_{n[r]}^2$ and $\sigma_{n[d]}^2$. The expression for the outage probability, p_{out} in (12), seems similar for both the TSR and PSR protocols. However, this is not the case because the final expressions for p_{out} are written in terms of constants a , b , c , and d , which differ in the TSR and PSR protocols

2) *Delay-Tolerant Transmission*: Since $T/2$ is the effective communication time between source and destination nodes in the block of time T seconds, as shown in Fig. 3(a), the throughput, τ at the destination node in delay-tolerant transmission mode is given by

$$\tau = C \frac{T/2}{T} = \frac{C}{2}, \quad (29)$$

where the ergodic capacity, C can be calculated using Proposition 4 (see below) for γ_D given in (26).

³The detailed derivation of p_{out} for the PSR protocol is omitted here because it follows the same steps as given in Appendix A.

Proposition 4: For the PSR protocol, C can be analytically calculated using (16), where⁴

$$a \triangleq P_s d_1^m d_2^m \sigma_{n[d]}^2 \gamma (1 - \rho), \quad (30a)$$

$$b \triangleq d_1^{2m} d_2^m \sigma_{n[r]}^2 \sigma_{n[d]}^2 \gamma, \quad (30b)$$

$$c \triangleq \eta P_s^2 \rho (1 - \rho), \quad (30c)$$

$$d \triangleq \eta P_s d_1^m \sigma_{n[r]}^2 \gamma \rho, \quad \text{and} \quad (30d)$$

$$u \triangleq \sqrt{\frac{4a}{c\lambda_h\lambda_g}}. \quad (30e)$$

The derived formulae for throughput for both the TSR and PSR protocols are summarized in Table I. The ergodic capacity, C in (16), has been expressed in terms of the constants a , b , c , and d , which differ in the TSR and PSR protocols and are defined in Table I.

Remark 1: It is important to mention here that, as shown in Table I, the final expressions for the throughput, τ at the destination node depend either on the outage probability, p_{out} , (delay-limited transmission) or the ergodic capacity, C , (delay-tolerant transmission), which in turn depend on energy harvesting time, α for the TSR protocol and power splitting factor, ρ for the PSR protocol.

It is desirable to find the values of α and ρ , that result in the maximum value of throughput, τ , for the TSR and PSR protocols, respectively. Because of the integrations and the Bessel functions involved in the analytical expressions of p_{out} and C , as shown in Table I, it seems intractable to evaluate closed-form expressions for the optimal value of α and ρ in terms of τ . However, the optimization can be done offline by numerically evaluating the optimal values of α and ρ for the given system parameters, including, source power P_s , energy harvesting efficiency η , source to relay distance d_1 , relay to destination distance d_2 , source transmission rate R , and noise variances $\sigma_{n[r]}^2$ and $\sigma_{n[d]}^2$.

V. NUMERICAL RESULTS AND DISCUSSION

This section uses the derived analytical results to obtain insights into the various design choices. The optimal value of throughput τ , optimal value of energy harvesting time α in the TSR protocol, and optimal value of power splitting ratio ρ in the PSR protocol are investigated for different values of noise

⁴The detailed derivation of C for the PSR protocol is omitted here because it follows the same steps as given in Appendix B.

TABLE I
THROUGHPUT (τ) FOR THE TSR AND PSR PROTOCOLS WITH AMPLIFY AND FORWARD RELAYING.

	TSR Protocol	PSR Protocol
	$\gamma^D = \frac{2\eta P_s^2 h ^4 g ^2 \alpha}{2\eta P_s h ^2 g ^2 d_1^m \sigma_{n[r]}^2 \alpha + P_s h ^2 d_1^m d_2^m \sigma_{n[d]}^2 (1 - \alpha) + d_1^{2m} d_2^m \sigma_{n[r]}^2 \sigma_{n[d]}^2 (1 - \alpha)}$ $\sigma_{n[r]}^2 = \sigma_{n_a}^2 + \sigma_{n_c}^2$ $\sigma_{n[d]}^2 = \sigma_{n_a}^2 + \sigma_{n_c}^2$ $u = \sqrt{\frac{4a}{c\lambda_h \lambda_g}}$	$\gamma^D = \frac{\eta P_s^2 h ^4 g ^2 \rho (1 - \rho)}{\eta P_s h ^2 g ^2 d_1^m \sigma_{n[r]}^2 \rho + P_s h ^2 d_1^m d_2^m \sigma_{n[d]}^2 (1 - \rho) + d_1^{2m} d_2^m \sigma_{n[r]}^2 \sigma_{n[d]}^2}$ $\sigma_{n[r]}^2 = (1 - \rho) \sigma_{n_a}^2 + \sigma_{n_c}^2$ $\sigma_{n[d]}^2 = \sigma_{n_a}^2 + \sigma_{n_c}^2$ $u = \sqrt{\frac{4a}{c\lambda_h \lambda_g}}$
Delay-Limited Transmission Mode	$p_{\text{out}} = 1 - \frac{1}{\lambda_h} \int_{z=d/c}^{\infty} e^{-\left(\frac{z}{\lambda_h} + \frac{az+b}{(cz^2-dz)\lambda_g}\right)} dz \text{ (Analytical)}$ $p_{\text{out}} \approx 1 - e^{-\frac{d}{c\lambda_h}} u K_1(u) \text{ (Analytical Approximation)}$	
	$\tau = (1 - p_{\text{out}})(1 - \alpha)R/2$ $a = P_s d_1^m d_2^m \sigma_{n[d]}^2 \gamma_0 (1 - \alpha)$ $b = d_1^{2m} d_2^m \sigma_{n[r]}^2 \sigma_{n[d]}^2 \gamma_0 (1 - \alpha)$ $c = 2\eta P_s^2 \alpha$ $d = 2\eta P_s d_1^m \sigma_{n[r]}^2 \gamma_0 \alpha$	$\tau = (1 - p_{\text{out}})R/2$ $a = P_s d_1^m d_2^m \sigma_{n[d]}^2 \gamma_0 (1 - \rho)$ $b = d_1^{2m} d_2^m \sigma_{n[r]}^2 \sigma_{n[d]}^2 \gamma_0$ $c = \eta P_s^2 \rho (1 - \rho)$ $d = \eta P_s d_1^m \sigma_{n[r]}^2 \gamma_0 \rho$
Delay-Tolerant Transmission Mode	$C = \int_{\gamma=0}^{\infty} \int_{z=d/c}^{\infty} \frac{(az+b)cz^2}{(cz^2-dz)^2 \lambda_g \lambda_h \gamma} e^{-\left(\frac{z}{\lambda_h} + \frac{az+b}{(cz^2-dz)\lambda_g}\right)} \log_2(1 + \gamma) dz d\gamma \text{ (Analytical)}$ $C \approx \int_{\gamma=0}^{\infty} \left(\frac{u^2 K_0(u) e^{-\frac{d}{c\lambda_h}}}{2\gamma} + \frac{du K_1(u) e^{-\frac{d}{c\lambda_h}}}{\gamma c \lambda_h} \right) \log_2(1 + \gamma) d\gamma \text{ (Analytical Approximation)}$	
	$\tau = (1 - \alpha)C/2$ $a = P_s d_1^m d_2^m \sigma_{n[d]}^2 \gamma (1 - \alpha)$ $b = d_1^{2m} d_2^m \sigma_{n[r]}^2 \sigma_{n[d]}^2 \gamma (1 - \alpha)$ $c = 2\eta P_s^2 \alpha$ $d = 2\eta P_s d_1^m \sigma_{n[r]}^2 \gamma \alpha$	$\tau = C/2$ $a = P_s d_1^m d_2^m \sigma_{n[d]}^2 \gamma (1 - \rho)$ $b = d_1^{2m} d_2^m \sigma_{n[r]}^2 \sigma_{n[d]}^2 \gamma$ $c = \eta P_s^2 \rho (1 - \rho)$ $d = \eta P_s d_1^m \sigma_{n[r]}^2 \gamma \rho$

variances, source to relay and relay to destination distances, d_1 and d_2 , respectively, source transmission rate, R and energy harvesting efficiency, η . The optimal values values of α and ρ are numerically obtained as explained in Remark 1. Note that the optimal values of α and ρ are defined as those values, which result in the maximum throughput τ at the destination node.

Unless otherwise stated, we set the distances $d_1 = d_2 = 1$ meter, source transmission rate, $R = 3$ bits/sec/Hz in delay limited transmission mode, energy harvesting efficiency, $\eta = 1$, source transmission

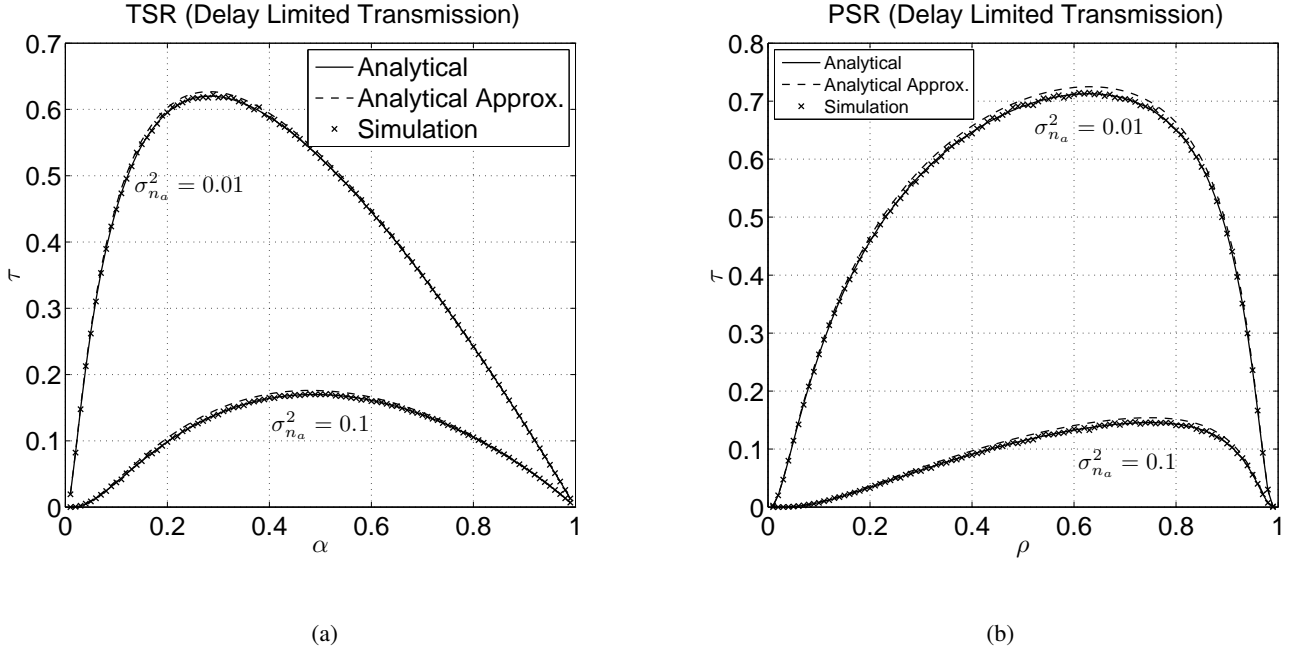


Fig. 4. Throughput τ at the destination node in delay-limited transmission mode with respect to (a) α for the TSR protocol and (b) ρ for the PSR protocol. Other parameters: $\sigma_{n_a}^2 = [0.1, 0.01]$, $\sigma_{n_c}^2 = 0.01$, $P_s = 1$, $\eta = 1$, $d_1 = d_2 = 1$, and $R = 3$.

power, $P_s = 1$ Joules/sec and path loss exponent $m = 2.7$ (corresponds to an urban cellular network environment [22]). For simplicity, similar noise variances at the relay and destination nodes are assumed, i.e., antenna noise variance, $\sigma_{n_a}^2 \triangleq \sigma_{n_a^{[r]}}^2 = \sigma_{n_a^{[d]}}^2$ and conversion noise variance, $\sigma_{n_c}^2 \triangleq \sigma_{n_c^{[r]}}^2 = \sigma_{n_c^{[d]}}^2$. The mean values, λ_h and λ_g , of the exponential random variables $|h|^2$ and $|g|^2$, respectively, are set to 1.

A. Verification of Analytical Results

In this subsection, for both the TSR and PSR protocols in delay-limited and delay-tolerant transmission modes, the analytical results for the throughput, τ , as shown in Table I, are examined and verified through simulations. Note that in order to calculate τ , the analytical results for p_{out} and C are evaluated using (12) and (16), respectively and the simulation results for p_{out} and C are obtained using (11) and (15), respectively. The simulation results in (11) and (15) are obtained by averaging these expressions over 10^5 realizations of Rayleigh fading channels h and g .

Fig. 4 plots the throughput τ in delay-limited transmission mode with respect to $0 < \alpha < 1$ for the TSR protocol (see Fig. 4(a)) and $0 < \rho < 1$ for the PSR protocol (see Fig. 4(b)). Different antenna noise variances, $\sigma_{n_a}^2 = [0.1, 0.01]$ are considered, while the conversion noise variance is kept fixed, i.e., $\sigma_{n_c}^2 = 0.01$. Source transmission rate is kept fixed at, $R = 3$ bits/sec/Hz. Fig. 4 uses the analytical and the

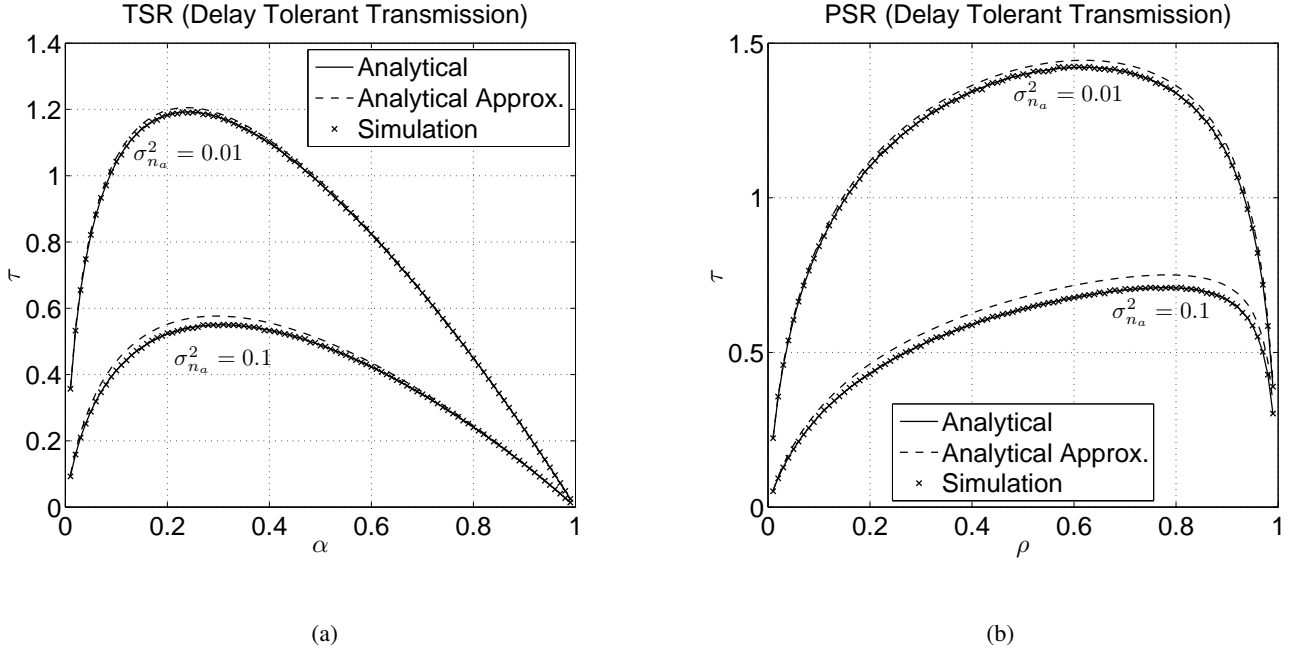


Fig. 5. Throughput τ at the destination node in delay-tolerant transmission mode with respect to (a) α for the TSR protocol and (b) ρ for the PSR protocol. Other parameters: $\sigma_{n_a}^2 = [0.1, 0.01]$, $\sigma_{n_c}^2 = 0.01$, $P_s = 1$, $\eta = 1$, and $d_1 = d_2 = 1$

analytical approximation (defined in figure as “Analytical Approx.”) expressions for outage probability, p_{out} , as summarized in Table I, in order to evaluate the throughput. It can be observed from Fig. 4 that analytical and simulation results match for all possible values of α and ρ . This verifies the analytical expression for p_{out} presented in *Proposition 1*. Moreover, Fig. 4 shows that the closed-form analytical approximation results are very close to the exact analytical results.

Fig. 5 plots the throughput τ in delay-tolerant transmission mode with respect to $0 < \alpha < 1$ for the TSR protocol (see Fig. 5(a)) and $0 < \rho < 1$ for the PSR protocol (see Fig. 5(b)). Similar to the delay-limited transmission case, different antenna noise variances, $\sigma_{n_a}^2 = [0.1, 0.01]$ are considered, while the conversion noise variance is kept fixed, i.e., $\sigma_{n_c}^2 = 0.01$. Fig. 5 uses the analytical and the analytical approximation (defined in figure as “Analytical Approx.”) expressions for ergodic capacity, C , as summarized in Table I, in order to evaluate τ . It can be observed from Fig. 5 that analytical and simulation results match for all possible values of α and ρ . This verifies the analytical expression for C presented in *Proposition 2*. Moreover, Fig. 5 shows very close results of the throughput for the approximated and exact expressions of C . The analytical approximation result of throughput deviates more from the exact analytical result at high noise variance, $\sigma_{n_a}^2 = 0.1$. This is because high SNR approximation is used in analytical approximation results.

B. Effect of Energy Harvesting Time, α (TSR protocol) and Power Splitting Factor, ρ (PSR protocol)

Fig. 4(a) shows that for the TSR protocol, throughput increases as α increases from 0 to some optimal α (0.28 for $\sigma_{n_a}^2 = 0.01$) but later, it starts decreasing as α increases from its optimal value. This is because for the values of α smaller than the optimal α , there is less time for energy harvesting. Consequently, less energy is harvested and small values of throughput are observed at the destination node due to large outage probability (see (14)). On the other hand, for the values of α greater than the optimal α , more time is wasted on energy harvesting and less time is available for information transmission. As a result, smaller throughput yields at the destination node due to small value of $(1 - \alpha)/2$ (see (14)).

Similarly, it can be observed from Fig. 4(b) that for the PSR protocol, throughput increases as ρ increases from 0 to some optimal ρ (0.63 for $\sigma_{n_a}^2 = 0.01$) but later, it starts decreasing as ρ increases from its optimal value. This is because for the values of ρ smaller than the optimal ρ , there is less power available for energy harvesting. Consequently, less transmission power P_r is available from the relay node and small values of throughput are observed at the destination node due to large outage probability (see (27)). On the other hand, for the values of ρ greater than the optimal ρ , more power is wasted on energy harvesting and less power is left for source to relay information transmission. As a result, poor signal strength is observed at the relay node and when the relay amplifies and forwards that noisy signal to the destination, more outage occurs and lesser throughput results at the destination node.

Fig. 5 shows the similar trends for the throughput in delay-tolerant transmission mode, as observed and explained for delay-limited transmission mode in Fig. 4. Thus, the same explanations hold here for the delay-tolerant transmission mode.

C. Effect of Noise Power

Fig. 6 plots the optimal throughput τ and optimal values of α and ρ for the TSR and PSR protocols, respectively, in delay-limited transmission mode for different values of antenna noise variance, $\sigma_{n_a}^2$ (see Fig. 6(a) for fixed $\sigma_{n_c}^2 = 0.01$) and for different values of conversion noise variance, $\sigma_{n_c}^2$ (see Fig. 6(b) for fixed $\sigma_{n_a}^2 = 0.01$). *It can be observed from Fig. 6 that the PSR protocol is better than the TSR protocol to obtain larger values of the throughput, except at relatively large noise variance, where the TSR protocol*

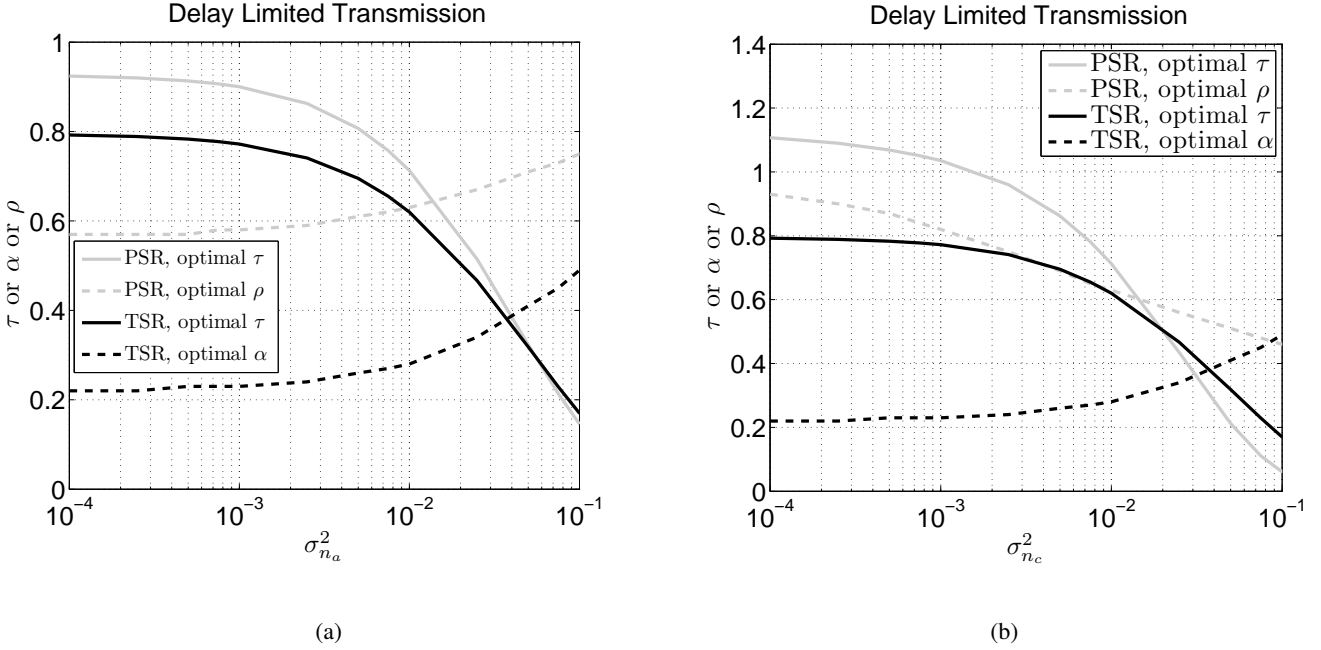


Fig. 6. Optimal throughput τ and optimal values of α and ρ for the TSR and PSR protocols, respectively, in delay-limited transmission mode for (a) different values of antenna noise variance $\sigma_{n_a}^2$ and $\sigma_{n_c}^2 = 0.01$ (fixed) and (b) different values of conversion noise variance $\sigma_{n_c}^2$ and $\sigma_{n_a}^2 = 0.01$ (fixed). Other parameters: $P_s = 1$, $\eta = 1$, $d_1 = d_2 = 1$, and $R = 3$ and p_{out} is given in (12a).

renders more throughput than the PSR protocol. Particularly, the crossover between the performances of the PSR and TSR protocols occurs at $\sigma_{n_a}^2 = 0.06$ (Fig. 6(a)) and $\sigma_{n_c}^2 = 0.02$ (Fig. 6(b)). Fig. 6(a) also shows that the optimal value of α and ρ increases by increasing $\sigma_{n_a}^2$. This is because for large values of antenna noise variances $\sigma_{n_a}^2$, more harvested energy E_h and consequently more energy harvesting time τ or more power splitting ratio ρ is required to avoid outage. However, unlike the results in Fig. 6(a), Fig. 6(b) shows that for the PSR protocol, optimal value of ρ decreases by increasing $\sigma_{n_c}^2$. This is because the input to the information receiver in the PSR protocol, as shown in Fig. 3(b), is $\sqrt{1 - \rho}y(t)$. Now, increasing the noise $n_c^{[r]}(t)$ requires more signal strength at the input of information receiver to avoid outage, which yields smaller values of optimal ρ with the increase of $\sigma_{n_c}^2$.

Fig. 7 plots the optimal throughput τ and optimal values of α and ρ for the TSR and PSR protocols, respectively, in delay-tolerant transmission mode for different values of antenna noise variance, $\sigma_{n_a}^2$ (see Fig. 7(a) for fixed $\sigma_{n_c}^2 = 0.01$) and for different values of conversion noise variance, $\sigma_{n_c}^2$ (see Fig. 7(b) for fixed $\sigma_{n_a}^2 = 0.01$). It can be observed from Fig. 7 that in the case of delay-tolerant transmission mode, the PSR protocol is recommended over the TSR protocol for the considered values of noise variance to obtain larger values of the throughput. Finally, Fig. 7 shows that similar trends for optimal value of α and ρ are

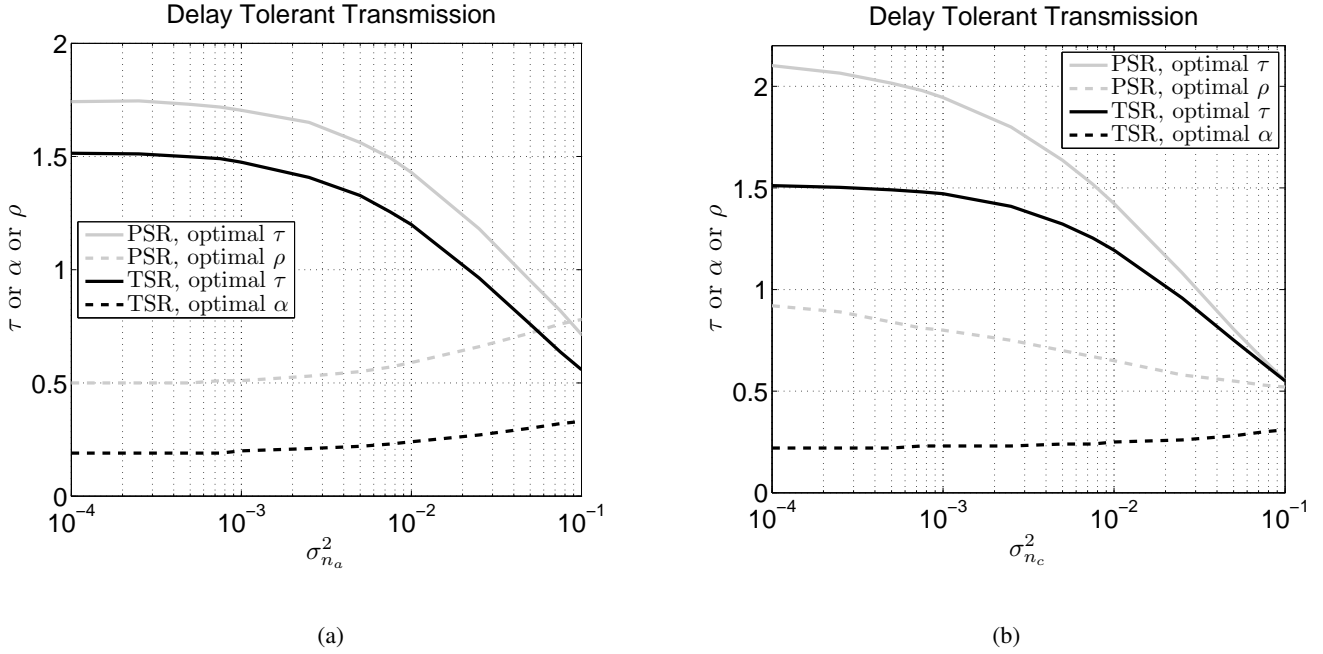


Fig. 7. Optimal throughput τ and optimal values of α and ρ for the TSR and PSR protocols, respectively, in delay-tolerant transmission mode for (a) different values of antenna noise variance $\sigma_{n_a}^2$ and $\sigma_{n_c}^2 = 0.01$ (fixed) and (b) different values of conversion noise variance $\sigma_{n_c}^2$ and $\sigma_{n_a}^2 = 0.01$ (fixed). Other parameters: $P_s = 1$, $\eta = 1$, $d_1 = d_2 = 1$ and C is given in (16a).

observed in delay-tolerant transmission mode, as were observed in Fig. 6 for delay-limited transmission mode.

D. Effect of Relay Location

Fig. 8 plots the optimal throughput τ and optimal values of α and ρ for the TSR and PSR protocols, respectively, in delay-limited transmission mode (see Fig. 8(a)) and delay-tolerant transmission mode (see Fig. 8(b)) for different values of source to relay distance, d_1 . The relay to destination distance, d_2 is set to $d_2 = 2 - d_1$ and the noise variances are kept fixed, i.e., $\sigma_{n_a}^2 = 0.01$ and $\sigma_{n_c}^2 = 0.01$. It can be observed from Fig. 8 that for both the TSR and PSR protocols, optimal throughput τ decreases as d_1 increases, i.e., as the distance between source node and the relay node increases. This is because by increasing d_1 , both energy harvested (E_h defined in (2) for the TSR protocol and defined in (19) for the PSR protocol) and received signal strength at the relay node ($y_r(k)$ defined in (3) for the TSR protocol and defined in (20) for the PSR protocol) decrease due to larger path loss, d_1^m . Consequently, the received signal strength at the destination node (γ_D defined in (10) for the TSR protocol and defined in (26) for the PSR protocol) is poor and the achievable throughput is decreased. However, the throughput does not much

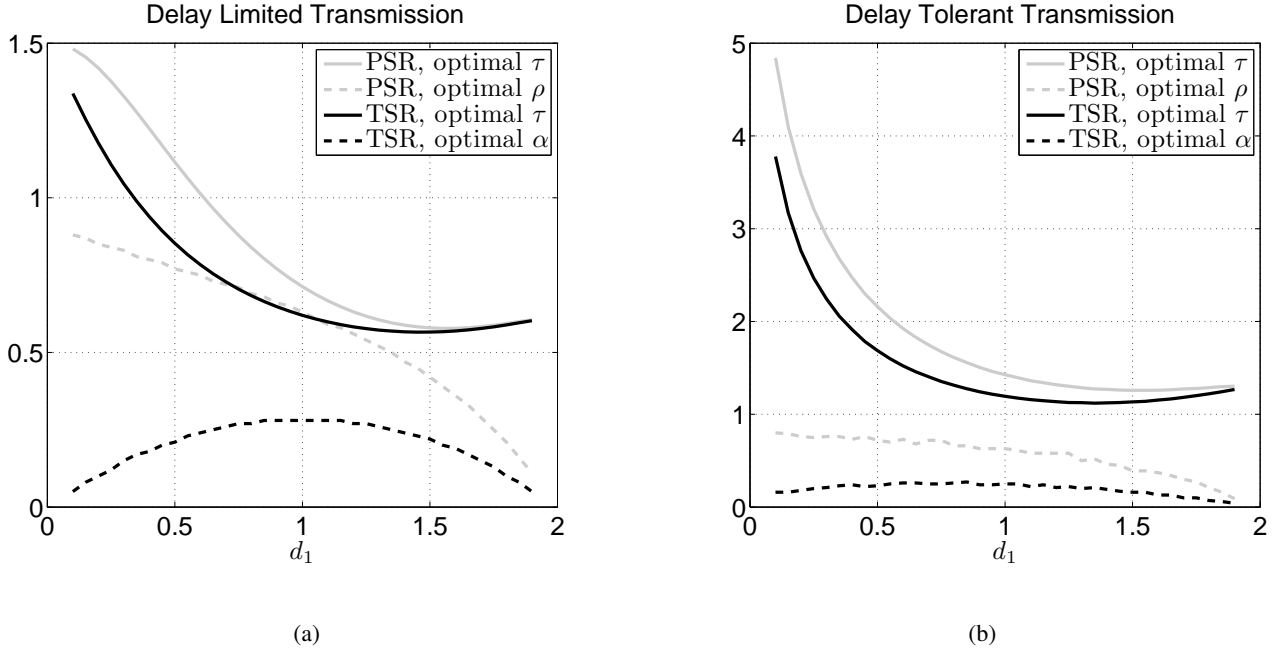


Fig. 8. Optimal throughput τ and optimal values of α and ρ for the TSR and PSR protocols, respectively, in (a) delay-limited transmission mode (p_{out} given in (12a)) and (b) delay-tolerant transmission mode (C given in (16a)), for different values of source to relay distance, d_1 . Other parameters: $\sigma_{n_a}^2 = 0.01$, $\sigma_{n_c}^2 = 0.01$, $P_s = 1$, $\eta = 1$, and $d_2 = 2 - d_1$.

change by increasing d_1 beyond 1.2 meters. This is because as the relay node gets closer to the destination ($d_2 < 0.8$), even lesser values of harvested energy, E_h suffice for reliable communication between relay and destination nodes due to smaller values of the relay to destination path loss, d_2^m . *It is important to note that, as illustrated in Fig. 8, the optimal relay location with energy harvesting is close to the source node. This is different from the general case where energy harvesting is not considered at the relay and maximum throughput is achieved when relay is in the mid-way between the source and the destination nodes.*⁵

Fig. 8(a) also shows that the optimal value of α in the TSR protocol is maximum at $d_1 = d_2 = 1$ i.e., when relay node is in the mid-way between source and destination nodes. The optimal α decreases if $d_1 < 1$ or $d_1 > 1$ for the TSR protocol. This is because if $d_1 > 1$, relay node gets closer to the destination node and small value of energy harvesting time α , or consequently small value of harvested energy E_h , is sufficient to achieve reliable communication between relay and destination nodes. On the other hand if $d_1 < 1$, relay node gets closer to the source node and smaller path loss d_1^m achieves large harvested energy E_h (see (2)) even for smaller energy harvesting time α . For the PSR protocol, Fig. 8(a)

⁵This is observed through simulations for non energy harvesting setup. The results, however, are not included here due to brevity.

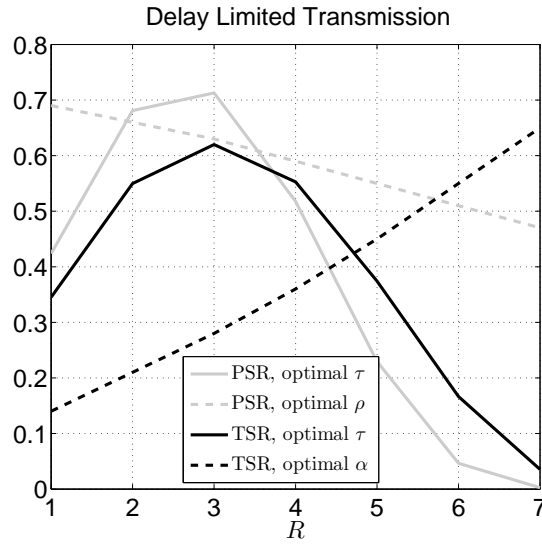


Fig. 9. Optimal throughput τ and optimal values of α and ρ for the TSR and PSR protocols, respectively, in delay-limited transmission mode for different values of source transmission rate, R . Other parameters: $\sigma_{n_a}^2 = 0.01$, $\sigma_{n_c}^2 = 0.01$, $P_s = 1$, $\eta = 1$, $d_1 = d_2 = 1$, and p_{out} is given in (12a).

shows that optimal value of ρ decreases as d_1 increases because in order to encounter smaller relay to destination path loss d_2^m (d_2 is increasing by decreasing d_1), small fraction of the source power, ρ for energy harvesting suffices reliable communication, that can avoid outage, between relay and destination nodes. Similar trends for optimal value of α and ρ are observed in delay-tolerant transmission mode in Fig. 8(b).

E. Effect of Source Transmission Rate in Delay-Limited Transmission

Fig. 9 plots the optimal throughput τ and optimal values of α and ρ for the TSR and PSR protocols, respectively, in delay-limited transmission mode for different values of source transmission rate, R bits/sec/Hz. Noise variances are kept fixed, i.e., $\sigma_{n_a}^2 = 0.01$ and $\sigma_{n_c}^2 = 0.01$. Fig. 9 shows that optimal τ increases as R increases to a certain value but then starts decreasing for larger values of R . This is because the throughput depends on R (see (14) for the TSR protocol and (27) for the PSR protocol) and thus at relatively low transmission rates, throughput decreases. On the other hand, for larger transmission rates R , receiver fails to correctly decode large amount of data in limited time. Thus, probability of outage p_{out} increases and throughput decreases. *It can be observed from Fig. 9 that the PSR protocol results in more throughput than the TSR protocol at relatively low transmission rates. On the other hand, when*

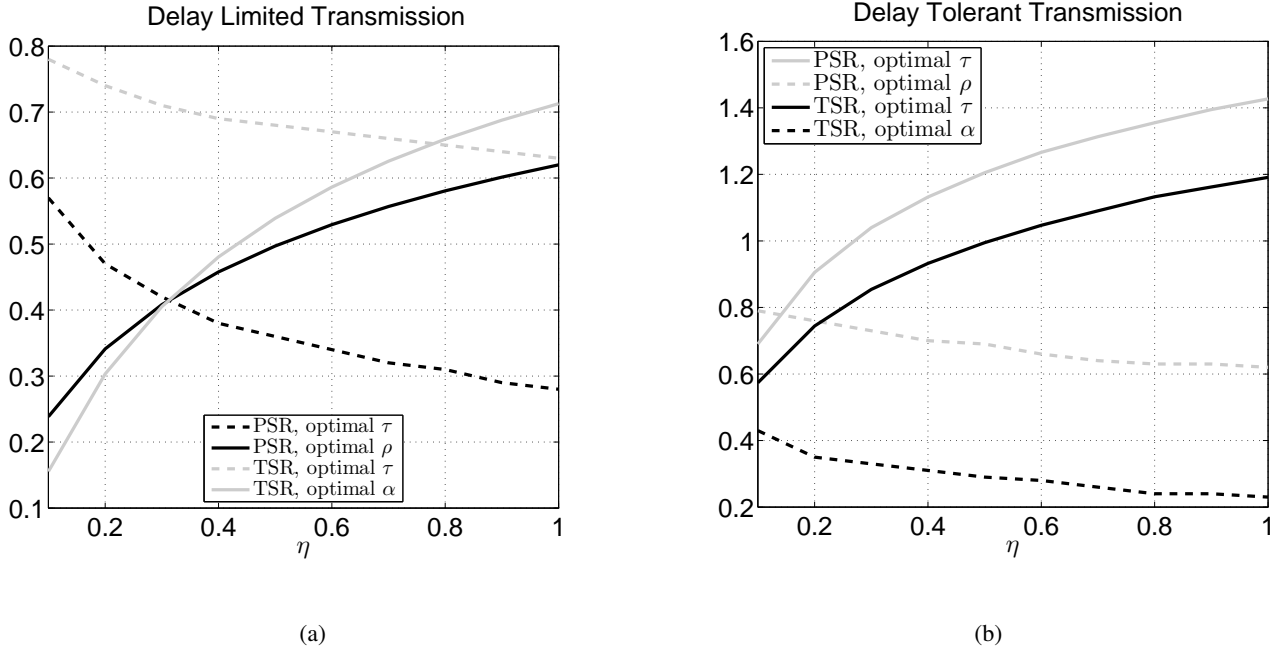


Fig. 10. Optimal throughput τ and optimal values of α and ρ for the TSR and PSR protocols, respectively, in (a) delay-limited transmission mode (p_{out} given in (12a)) and (b) delay-tolerant transmission mode (C given in (16a)), for different values of energy harvesting efficiency, η . Other parameters: $\sigma_{n_a}^2 = 0.01$, $\sigma_{n_c}^2 = 0.01$, $P_s = 1$, and $d_1 = d_2 = 1$.

transmitting at larger rates, the TSR protocol renders larger values of throughput compared to the PSR protocol.

Fig. 9 shows that the optimal value of α increases by increasing the transmission rate R in the TSR protocol. This is because as the transmission rate increases, threshold SNR γ_0 increases, and larger value of harvested energy (or energy harvesting time α) is required to avoid outage at the destination node. On the other hand, it can be observed from Fig. 9 that the optimal value of the fractional power ρ going into the energy harvesting receiver decreases by increasing the transmission rate R in the PSR protocol. This is because as the transmission rate increases, more power is required for the information receiver at the relay node in order to cope with the large amount of data and avoid outage. Thus, more power for information receiver means larger values of $1 - \rho$ (see Fig. 3(b)), which decreases ρ with the increase of R .

F. Effect of Energy Harvesting Efficiency

Fig. 10 plots the optimal throughput τ and optimal values of α and ρ for the TSR and PSR protocols, respectively, in delay-limited transmission mode (see Fig. 10(a)) and delay-tolerant transmission mode

(see Fig. 10(b)) for different values of energy harvesting efficiency, η . *It can be observed from Fig. 10(a) that for smaller values of energy harvesting efficiency η , the TSR protocol outperforms the PSR protocol in terms of throughput. On the other hand, Fig. 10(b) shows that in delay-tolerant transmission mode, the PSR protocol outperforms the TSR protocol for all the values of η .* Moreover, Fig. 10 shows that both optimal value of α in the TSR protocol and the optimal value of ρ in the PSR protocol decrease by increasing η . This is obvious because poor energy harvesting efficiency (smaller values of η) requires more energy harvesting time α in the TSR protocol and require more power splitting ratio ρ in the PSR protocol to avoid outage (delay-limited transmission mode) or to achieve reliable decoding with capacity codes (delay-tolerant transmission mode).

VI. CONCLUSIONS

In this paper, an amplify-and-forward wireless cooperative or sensor network has been considered, where an energy constrained relay node harvests energy from the received RF signal and uses that harvested energy to forward the source signal to the destination node. Two relaying protocols, namely, i) TSR protocol and ii) PSR protocol, are proposed to enable wireless energy harvesting and information processing at the relay, based on the recently developed TS and PS receiver architectures. Both delay-limited and delay-tolerant transmission modes are considered for communication. In order to determine the achievable throughput at the destination, analytical expressions for the outage probability and the ergodic capacity are derived for delay-limited and delay-tolerant transmission modes, respectively. The optimal value of energy harvesting time in the TSR protocol and the optimal value of power splitting ratio in the PSR protocol are numerically investigated. The numerical analysis in this paper has provided practical insights into the effect of various system parameters, such as energy harvesting time, power splitting ratio, source transmission rate, source to relay distance, noise power, and energy harvesting efficiency, on the performance of wireless energy harvesting and information processing using AF relay nodes. The numerical analysis in this paper is underpinned by the derived analytical expressions for the throughput for both TSR and PSR protocols, which are summarized in Table I,

APPENDIX A

PROOF OF PROPOSITION 1 IN (12)

This appendix derives the p_{out} , in (12), at the destination node for the TSR protocol. Substituting (10) into (11), p_{out} is given by

$$\begin{aligned}
 p_{\text{out}} &= p \left(\frac{2\eta P_s^2 |h|^4 |g|^2 \alpha}{2\eta P_s |h|^2 |g|^2 d_1^m \sigma_{n[r]}^2 \alpha + P_s |h|^2 d_1^m d_2^m \sigma_{n[d]}^2 (1 - \alpha) + d_1^{2m} d_2^m \sigma_{n[r]}^2 \sigma_{n[d]}^2 (1 - \alpha)} < \gamma_0 \right) \\
 &= p \left(|g|^2 < \frac{P_s d_1^m d_2^m \sigma_{n[d]}^2 \gamma_0 (1 - \alpha) |h|^2 + d_1^{2m} d_2^m \sigma_{n[r]}^2 \sigma_{n[d]}^2 \gamma_0 (1 - \alpha)}{2\eta P_s^2 \alpha |h|^4 - 2\eta P_s d_1^m \sigma_{n[r]}^2 \gamma_0 \alpha |h|^2} \right) \\
 &= p \left(|g|^2 < \frac{a|h|^2 + b}{c|h|^4 - d|h|^2} \right)
 \end{aligned} \tag{A.1}$$

where $a \triangleq P_s d_1^m d_2^m \sigma_{n[d]}^2 \gamma_0 (1 - \alpha)$, $b \triangleq d_1^{2m} d_2^m \sigma_{n[r]}^2 \sigma_{n[d]}^2 \gamma_0 (1 - \alpha)$, $c \triangleq 2\eta P_s^2 \alpha$, and $d \triangleq 2\eta P_s d_1^m \sigma_{n[r]}^2 \gamma_0 \alpha$.

Given the factor in the denominator, $c|h|^4 - d|h|^2$, can be positive or negative, p_{out} is given by

$$\begin{aligned}
 p_{\text{out}} &= p \left((c|h|^4 - d|h|^2) |g|^2 < (a|h|^2 + b) \right) \\
 &= \begin{cases} p \left(|g|^2 < \frac{a|h|^2 + b}{c|h|^4 - d|h|^2} \right), & |h|^2 < d/c \\ p \left(|g|^2 > \frac{a|h|^2 + b}{c|h|^4 - d|h|^2} \right) = 1, & |h|^2 > d/c \end{cases}
 \end{aligned} \tag{A.2}$$

The second equality in (A.2) follows due to the fact that if $|h|^2 > d/c$, $c|h|^4 - d|h|^2$ will be a negative number and probability of $|g|^2$ being greater than some negative number is always 1. Following (A.2), p_{out} is given by

$$\begin{aligned}
 p_{\text{out}} &= \int_{z=0}^{d/c} f_{|h|^2}(z) p \left(|g|^2 > \frac{az + b}{cz^2 - dz} \right) dz + \int_{z=d/c}^{\infty} f_{|h|^2}(z) p \left(|g|^2 < \frac{az + b}{cz^2 - dz} \right) dz \\
 &= \int_{z=0}^{d/c} f_{|h|^2}(z) dz + \int_{z=d/c}^{\infty} f_{|h|^2}(z) \left(1 - e^{-\frac{az+b}{(cz^2-dz)\lambda_g}} \right) dz
 \end{aligned} \tag{A.3}$$

where z is the integration variable, $f_{|h|^2}(z) \triangleq \frac{1}{\lambda_h} e^{-z/\lambda_h}$ is the probability density function (PDF) of exponential random variable $|h|^2$, λ_h is the mean of the exponential random variable $|h|^2$, $F_{|g|^2}(z) \triangleq p(|g|^2 < z) = 1 - e^{-z/\lambda_g}$ is the cumulative distribution function (CDF) of the exponential random variable $|g|^2$ and λ_g is the mean of the exponential random variable $|g|^2$. Substituting $f_{|h|^2}(z) = \frac{1}{\lambda_h} e^{-z/\lambda_h}$ in (A.3),

p_{out} is given by

$$p_{\text{out}} = 1 - \frac{1}{\lambda_h} \int_{z=d/c}^{\infty} e^{-\left(\frac{z}{\lambda_h} + \frac{az+b}{(cz^2-dz)\lambda_g}\right)} dz \quad (\text{A.4})$$

(A.4) presents the analytical expression of p_{out} for the TSR protocol, as presented in Proposition 1 in (12).

The integration in (A.4) cannot be further simplified. However, one can apply a high SNR approximation and obtain further simplified expression for p_{out} . At high SNR, the third factor in the denominator of (10), $d_1^{2m} d_2^m \sigma_{n[r]}^2 \sigma_{n[d]}^2 (1 - \alpha)$, is negligible (because of the product of the two noise variance terms) compared to the other two factors in the denominator, $2\eta P_s |h|^2 |g|^2 d_1^m \sigma_{n[r]}^2 \alpha$ and $P_s |h|^2 d_1^m d_2^m \sigma_{n[d]}^2 (1 - \alpha)$, i.e., $\gamma_D \approx \frac{2\eta P_s^2 |h|^4 |g|^2 \alpha}{2\eta P_s |h|^2 |g|^2 d_1^m \sigma_{n[r]}^2 \alpha + P_s |h|^2 d_1^m d_2^m \sigma_{n[d]}^2 (1 - \alpha)}$. In other words, at high SNR, the constant b can be approximated by 0, i.e., $b = d_1^{2m} d_2^m \sigma_{n[r]}^2 \sigma_{n[d]}^2 \gamma_0 (1 - \alpha) \approx 0$. Thus, p_{out} in (A.4) can be approximated as

$$p_{\text{out}} \approx 1 - \frac{1}{\lambda_h} \int_{z=d/c}^{\infty} e^{-\left(\frac{z}{\lambda_h} + \frac{a}{(cz-d)\lambda_g}\right)} dz \quad (\text{A.5})$$

Let us define a new integration variable $x \triangleq cz - d$. Thus, approximated outage at high SNR is given by

$$\begin{aligned} p_{\text{out}} &\approx 1 - \frac{e^{-\frac{d}{c\lambda_h}}}{c\lambda_h} \int_{x=0}^{\infty} e^{-\left(\frac{x}{\lambda_h c} + \frac{a}{x\lambda_g}\right)} dx \\ &= 1 - e^{-\frac{d}{c\lambda_h}} u K_1(u) \end{aligned} \quad (\text{A.6})$$

where $u \triangleq \sqrt{\frac{4a}{c\lambda_h\lambda_g}}$, $K_1(\cdot)$ is the first-order modified Bessel function of the second kind [21] and the last equality is obtained by using the formula, $\int_0^{\infty} e^{-\frac{\beta}{4x} - \gamma x} dx = \sqrt{\frac{\beta}{\gamma}} K_1(\sqrt{\beta\gamma})$ [21, §3.324.1]. This ends the proof for Proposition 1.

APPENDIX B

PROOF OF PROPOSITION 2 IN (16)

In order to find the analytical expression for the ergodic capacity, the PDF of γ_D , $f_{\gamma_D}(\gamma)$, needs to be evaluated first. The PDF of γ_D can be obtained from the CDF of γ_D , $F_{\gamma_D}(\gamma)$ which is given by

$$F_{\gamma_D}(\gamma) = p(\gamma_D < \gamma) = 1 - \frac{1}{\lambda_h} \int_{z=d/c}^{\infty} e^{-\left(\frac{z}{\lambda_h} + \frac{az+b}{(cz^2-dz)\lambda_g}\right)} dz, \quad (\text{B.1})$$

where $a \triangleq P_s d_1^m d_2^m \sigma_{n[d]}^2 \gamma (1 - \alpha)$, $b \triangleq d_1^{2m} d_2^m \sigma_{n[r]}^2 \sigma_{n[d]}^2 \gamma (1 - \alpha)$, $c \triangleq 2\eta P_s^2 \alpha$, $d \triangleq 2\eta P_s d_1^m \sigma_{n[r]}^2 \gamma \alpha$, and equality in (B.1) follows from (11) and (12a). Using (B.1), the PDF of γ_D is given by

$$f_{\gamma_D}(\gamma) = \frac{\partial F_{\gamma_D}(\gamma)}{\partial \gamma} = \frac{1}{\lambda_h \gamma} \int_{z=d/c}^{\infty} \frac{(az+b)cz^2}{(cz^2-dz)^2 \lambda_g} e^{-\left(\frac{z}{\lambda_h} + \frac{az+b}{(cz^2-dz)\lambda_g}\right)} dz. \quad (\text{B.2})$$

Using (15) and the PDF $f_{\gamma_D}(\gamma)$ in (B.2), the ergodic capacity C is given by

$$C = \int_{\gamma=0}^{\infty} f_{\gamma_D}(\gamma) \log_2(1 + \gamma) d\gamma \quad (\text{B.3a})$$

$$= \int_{\gamma=0}^{\infty} \int_{z=d/c}^{\infty} \frac{(az+b)cz^2}{(cz^2-dz)^2 \lambda_g \lambda_h \gamma} e^{-\left(\frac{z}{\lambda_h} + \frac{az+b}{(cz^2-dz)\lambda_g}\right)} \log_2(1 + \gamma) dz d\gamma. \quad (\text{B.3b})$$

(B.3b) presents the analytical expression of C for the TSR protocol, as presented in Proposition 2 in (16).

The integration in (B.3b) cannot be further simplified. However, one can apply high SNR approximation, as explained earlier in Appendix A below (A.4), to further simplify the expression in (B.3b). Thus, using (B.1), the approximate value for the CDF of γ_D is given by

$$\begin{aligned} F_{\gamma_D}(\gamma) &\approx 1 - \frac{1}{\lambda_h} \int_{z=d/c}^{\infty} e^{-\left(\frac{z}{\lambda_h} + \frac{a}{(cz-d)\lambda_g}\right)} dz \\ &= 1 - e^{-\frac{d}{c\lambda_h}} u K_1(u), \end{aligned} \quad (\text{B.4})$$

where $u \triangleq \sqrt{\frac{4a}{c\lambda_h \lambda_g}}$, a , c , and d are defined below (B.1) and the second equality in (B.4) follows using (A.5)-(A.6). Evaluating the derivative of $F_{\gamma_D}(\gamma)$ in (B.4) with respect to γ , the PDF of γ_D can be approximated as

$$f_{\gamma_D}(\gamma) \approx \frac{u^2 K_0(u) e^{-\frac{d}{c\lambda_h}}}{2\gamma} + \frac{du K_1(u) e^{-\frac{d}{c\lambda_h}}}{\gamma c \lambda_h} \quad (\text{B.5})$$

where (B.5) follows from (B.4) using the property of Bessel function, $\frac{d}{dz}(z^v K_v(z)) = -z^v K_{v-1}(z)$ [21, §8.486.18]. Thus, using (B.3a) and (B.5), approximated ergodic capacity at high SNR is given by

$$C \approx \int_{\gamma=0}^{\infty} \left(\frac{u^2 K_0(u) e^{-\frac{d}{c\lambda_h}}}{2\gamma} + \frac{du K_1(u) e^{-\frac{d}{c\lambda_h}}}{\gamma c \lambda_h} \right) \log_2(1 + \gamma) d\gamma \quad (\text{B.6})$$

This ends the proof for Proposition 2.

REFERENCES

- [1] J. Xu and R. Zhang, "Throughput optimal policies for energy harvesting wireless transmitters with non-ideal circuit power," *submitted to IEEE J. Sel. Area. Comm.*, 2012. [Online]. Available: <http://arxiv.org/abs/1204.3818>
- [2] C. K. Ho and R. Zhang, "Optimal energy allocation for wireless communications with energy harvesting constraints," *IEEE Trans. Signal Process.*, vol. 60, no. 9, pp. 4808–4818, Sep. 2012.
- [3] S. Luo, R. Zhang, and T. J. Lim, "Optimal save-then-transmit protocol for energy harvesting wireless transmitters," *submitted to IEEE Trans. Wireless Commun.*, 2012. [Online]. Available: <http://arxiv.org/abs/1204.1240>
- [4] L. R. Varshney, "Transporting information and energy simultaneously," in *Proc. IEEE ISIT*, 2008.
- [5] P. Grover and A. Sahai, "Shannon meets Tesla: wireless information and power transfer," in *Proc. IEEE ISIT*, 2010.
- [6] X. Zhou, R. Zhang, and C. K. Ho, "Wireless information and power transfer: Architecture design and rate-energy tradeoff," 2012. [Online]. Available: <http://arxiv.org/abs/1205.0618>
- [7] A. M. Fouladgar and O. Simeone, "On the transfer of information and energy in multi-user systems," *accepted for publication in IEEE Commun. Lett.*, 2012.
- [8] B. K. Chalise, Y. D. Zhang, and M. G. Amin, "Energy harvesting in an OSTBC based amplify-and-forward MIMO relay system," in *Proc. IEEE ICASSP*, 2012.
- [9] K. Huang and V. K. N. Lau, "Enabling wireless power transfer in cellular networks: architecture, modeling and deployment," *submitted to IEEE J. Sel. Areas Commun.*, 2012. [Online]. Available: <http://arxiv.org/abs/1207.5640>
- [10] P. Popovski, A. M. Fouladgar, and O. Simeone, "Interactive joint transfer of energy and information," *ArXiv Technical Report*, 2012. [Online]. Available: <http://arxiv.org/abs/1209.6367>
- [11] L. Liu, R. Zhang, and K.-C. Chua, "Wireless information transfer with opportunistic energy harvesting," *accepted for publication in IEEE Trans. Wireless Commun.*, 2012. [Online]. Available: <http://arxiv.org/abs/1204.2035>
- [12] R. Zhang and C. K. Ho, "MIMO broadcasting for simultaneous wireless information and power transfer," *submitted to IEEE Trans. Wireless Commun.*, 2012. [Online]. Available: <http://arxiv.org/abs/1105.4999>
- [13] V. Raghunathan, S. Ganeriwal, and M. Srivastava, "Emerging techniques for long lived wireless sensor networks," *IEEE Commun. Mag.*, vol. 44, no. 4, pp. 108–114, Apr. 2006.
- [14] J. A. Paradiso and T. Starner, "Energy scavenging for mobile and wireless electronics," *IEEE Trans. Pervasive Comput.*, vol. 4, no. 1, p. 1827, Jan. 2005.
- [15] B. Medepally and N. B. Mehta, "Voluntary energy harvesting relays and selection in cooperative wireless networks," *IEEE Trans. Wireless Commun.*, vol. 9, no. 11, pp. 3543–3553, Nov. 2010.
- [16] Z. Xiang and M. Tao, "Robust beamforming for wireless information and power transmission," *IEEE Wireless Commun. Letters*, vol. 1, no. 4, pp. 372–375, 2012.
- [17] S. Lee, K. Huang, and R. Zhang, "Cognitive energy harvesting and transmission from a network perspective," in *Proc. IEEE ICCS*, 2012.

- [18] P. T. Venkata, S. N. A. U. Nambi, R. V. Prasad, and I. Niemegeers, "Bond graph modeling for energy-harvesting wireless sensor networks," *IEEE Computer Society*, vol. 45, no. 9, pp. 31–38, Sep. 2012.
- [19] M. O. Hasna and M.-S. Alouini, "Performance analysis of two-hop relayed transmissions over Rayleigh fading channels," in *Proc. IEEE VTC*, 2002.
- [20] J. N. Laneman, D. N. C. Tse, and G. W. Wornell, "Cooperative diversity in wireless networks: Efficient protocols and outage behavior," *IEEE Trans. Inf. Theory*, vol. 50, no. 12, pp. 3062–3080, Dec. 2004.
- [21] I. S. Gradshteyn and I. M. Ryzhik, *Table of integrals, series, and products*, 4, Ed. Academic Press, Inc., 1980.
- [22] H. Meyr, M. Moeneclaey, and S. A. Fechtel, *Digital Communication Receivers, Synchronization, Channel Estimation, and Signal Processing*, J. G. Proakis, Ed. Wiley Series in Telecom. and Signal Processing, 1998.